arXiv:1512.05328v2 [hep-ph] 13 Jan 2016

EFI-15-40

A pseudoscalar decaying to photon pairs in the early LHC Run 2 data

Matthew Low[a], Andrea Tesi[b], Lian-Tao Wang[c]

[a] *School of Natural Sciences, Institute for Advanced Study, Princeton, NJ 08540*

[b] *Department of Physics, Enrico Fermi Institute, University of Chicago, Chicago, IL 60637*

[c] *Department of Physics, Enrico Fermi Institute, and Kavli Institute for Cosmological Physics, University of Chicago, Chicago, IL 60637*

Abstract

In this paper we explore the possibility of a pseudoscalar resonance to account for the 750 GeV diphoton excess observed both at ATLAS and at CMS. We analyze the ingredients needed from the low energy perspective to obtain a sufficiently large diphoton rate to explain the signal while avoiding constraints from other channels. Additionally, we point out composite Higgs models in which one can naturally obtain a pseudoscalar at the 750 GeV mass scale and we estimate the pseudoscalar couplings to standard model particles that one would have in such models. A generic feature of models that can explain the excess is the presence of new particles in addition to the 750 GeV state. Finally, we note that due to the origin of the coupling of the resonance to photons, one expects to see comparable signals in the $Z\gamma$, ZZ, and WW channels.

E-mail: mattlow@ias.edu, atesi@uchicago.edu, liantaow@uchicago.edu

Contents

1 Motivation **1**

2 Signals and constraints from the LHC **2**

3 The interactions of a pseudoscalar **3**

4 The mass scale of a pseudoscalar **11**

5 Alternative explanations **16**
5.1 Scalar resonance 16
5.2 Spin-2 resonance 17

6 Conclusions **18**

A SO(6)/SO(5) model **19**
A.1 The gauge sector 19
A.2 The fermion sector 20

1 Motivation

With the start of the second run of the Large Hadron Collider (LHC), we are seeing the first glimpses into physics at collision energies of 13 TeV. So far ATLAS and CMS have only collected a small amount of data (3.2 fb^{-1} and 2.6 fb^{-1} respectively), but that is already enough to set competitive limits on certain classes of new particles. For instance, jets and missing energy searches are already setting stronger limits on gluinos than at 8 TeV, due to the quickly growing parton luminosities at high masses. For new particles at lower masses, however, the parton luminosity increase is much milder and in most cases the 13 TeV searches have not yet surpassed the 8 TeV searches in sensitivity.

One 13 TeV search that has received significant attention recently is the diphoton resonance search. Both ATLAS [1] and CMS [2] observe an excess at 750 GeV. It appears that the excess is compatible both with Run 1 data and between ATLAS and CMS which makes this a compelling case of potential new physics. In this paper we explore the model building possibilities to describe this excess from two complementary perspectives. The first perspective we take is to quantitatively analyze the low energy interactions needed to produce the observed diphoton rate. For this we identify the diphoton resonance as a new pseudoscalar particle that couples to the standard model (SM) through dimension 5 operators. The generic picture is that the pseudoscalar is produced in gluon fusion and then decays to a pair of photons. We show that this parametrization can account for the excess either with a large enhancement in the coupling to photons or with a moderate enhancement in the coupling to photons and gluons and moderate suppression in the couplings to fermions. Either of these cases implies that more particles in addition to the 750 GeV resonance are needed to fit the data.

The second aspect of the diphoton excess that we address is naturally finding a scalar (or pseudoscalar) with a mass of ∼750 GeV in a complete model. We know from the familiar example of the Higgs that theories with fundamental scalars appearing much below the cutoff are finetuned. One way this finetuning problem has been addressed is to posit that the Higgs is actually a composite particle of some new strong dynamics. While this idea solves the hierarchy problem in principle, in practice there is still residual tuning associated with a light Higgs meaning that we are forced to live with some level of tuning. It could be case, however, that there are other scalars coming from the strong dynamics that are not tuned. In other words, it could be that the Higgs as a pseudo Nambu Goldstone Boson (pNGB) is slightly tuned, but that the other pNGBs are at their naturalness limit. We will argue that in the composite Higgs framework one can have additional light scalars at the 750 GeV mass scale and that such (pseudo)scalars are compatible with the excess.

Given the minimal information about the diphoton resonance, one cannot conclusively associate the resonance to the pseudoscalar parametrization that we present. We therefore survey a few other model building possibilities along with a few simple estimates to assess how easily these alternative models can fit the excess in comparison to the pseudoscalar case. In particular we look at a scalar resonance and a spin-2 resonance.

The outline is as follows. In Sec. 2 we review the current experiment status of the diphoton resonance and collect limits from other potentially relevant channels. The interactions of a pseudoscalar are described in Sec. 3 along with computations of widths, branching ratios, and rates. In Sec. 4 we address the issue of getting the ∼750 GeV mass scale in composite Higgs models. To conclude, in Sec. 5 we point out other possibilities and summarize in Sec. 6. App. A provides details of the SO(6)/SO(5) composite Higgs model that contains a pseudoscalar pNGB.

2 Signals and constraints from the LHC

ATLAS and CMS have both reported excess in the diphoton channel at a mass very near to 750 GeV. For a narrow resonance, the local significance reported by ATLAS was 3.6σ and 2.6σ by CMS. When a wide resonance signal model is used, the significances shift to 3.9σ for ATLAS and 2.0σ for CMS. In both experiments the global significance is $\sim 2\sigma$.

To gain some idea of the expected sensitivity, we compile the expected and observed limits set by Run 1 diphoton searches in Table 1.

While a proper analysis should perform a combination of both the 8 TeV and 13 TeV results from both experiments to assess the compatibility of the signal and the correct cross section to fit, this is difficult to do reliably with such a small number of events. As such we will show the cross sections that can be obtained with a pseudoscalar resonance rather than fixing a signal strength value. As a guide, one can use the CMS combination of their 8 TeV and 13 TeV results which finds a cross section of $\sim 3-5$ fb [6].

In Table 2 we list the observed limits from other channels that can be applicable to models that explain the diphoton excess. The limits shown are the observed limits and are set on $\sigma \times \mathcal{BR}$. For dijet limits we use the reported acceptance of $\mathcal{A} = 0.6$ for spin-0 signals to cast the limit from

$\gamma\gamma$	expected	observed	
ATLAS (spin-2)	1.9 fb	2.4 fb	[3]
CMS (spin-2)	1.5 fb	1.9 fb	[4]
CMS (narrow)	0.7 fb	1.3 fb	[5]
CMS (wide)	2.0 fb	2.3 fb	[5]

Table 1. Upper limits (at 95% CL) on the $\sigma \times \mathcal{BR}$ of a 750 GeV resonance decaying to a pair of photons from 8 TeV LHC data.

$\sigma \times \mathcal{BR} \times \mathcal{A}$ to $\sigma \times \mathcal{BR}$ [16,17]. There are also searches for resonances in the $\tau^+\tau^-$ [22,23], Zh [24], and monojet [25,26] channels which can be relevant for particular models.

In Table 3 we rescale the strongest 8 TeV limits by their gg parton luminosity ratio [27] because in the models we consider the production is dominated by gluon fusion. A strict comparison of compatibility of a proposed model with 8 TeV limits would involve simulating the signal model at 8 TeV but the numbers in Table 3 offer a quick comparison.

Finally, we note that the observed signal rate of $\sim 3-5$ fb is rather large. In the case of the SM Higgs, the decays to photons are mediated by loops of tops and W's and lead to a diphoton branching ratio of $\sim 10^{-3}$. If the decays of the 750 GeV resonance to photons were likewise only mediated by tops and W's the diphoton ratio would be small, $\lesssim 10^{-4}$ (because WW and ZZ decays are now onshell), which would require rates to $t\bar{t}$ and WW of $\mathcal{O}$(pb) at Run 1. From Table 2 this is clearly ruled out. Thus one can conclude that for a sufficiently large diphoton rate the 750 GeV is not the only new particle, more are needed!

3 The interactions of a pseudoscalar

A spin-0 particle can either be a scalar or a pseudoscalar. The simplest possibility to start with is to consider an SM singlet. A scalar singlet can potentially mix with the Higgs which would introduce tree level decays to $t\bar{t}$, WW, ZZ and even hh, which can place strong constraints on the mixing. It also suppresses the rate to photons compared to VV similarly to the case of a heavy SM Higgs of mass 750 GeV. This very fact together with the relative importance of the diboson channels (see Table 3) requires a huge contribution to the diphoton rate from new physics or a tuning of the mixing. Assuming CP conservation, a pseudoscalar will not mix with the Higgs which makes explaining the excess easier.[1] We will therefore focus our discussion on a pseudoscalar resonance, and reserve comments on the scalar case until Sec. 5.

We consider the SM extended by the addition of an SM singlet pseudoscalar η which transforms under CP as

$$\eta \xrightarrow{\text{CP}} -\eta. \tag{1}$$

[1] A scalar as part of an additional doublet is another scenario that can be safe from mixing with the Higgs.

final state		observed	
$t\bar{t}$	scalar	700 fb	ATLAS [7]
$t\bar{t}$	spin-2	540 fb	ATLAS [7]
$t\bar{t}$	narrow	450 fb	CMS [8]
$t\bar{t}$	wide	510 fb	CMS [8]
$b\bar{b}$		1.2 pb	CMS [9]
$Z\gamma$		2.7 fb	ATLAS [10]
ZZ	scalar	12 fb	ATLAS [11]
ZZ	spin-2	38 fb	ATLAS [12]
ZZ	scalar	23 fb	CMS [13]
ZZ	spin-2	53 fb	CMS [14]
WW	spin-2	67 fb	ATLAS [15]
WW	scalar	47 fb	CMS [13]
jj	Gaussian	2.0 pb	ATLAS [16]
jj	Breit Wigner	20.0 pb	ATLAS [16]
jj		2.9 pb	CMS [17]
$\ell^+\ell^-$	spin-2	1.1 fb	ATLAS [18]
$\ell^+\ell^-$	spin-2	3.5 fb	CMS [19]
hh		32 fb	ATLAS [20]
hh	scalar	51 fb	CMS [21]
hh	spin-2	39 fb	CMS [21]

Table 2. Observed upper limits (at 95% CL) on $\sigma \times \mathcal{BR}$ of a 750 GeV resonance decaying to various final states from 8 TeV LHC data.

The scalar potential is given by

$$V = V_{\rm SM} + \frac{m_\eta^2}{2}\eta^2 + \frac{\lambda_\eta}{4!}\eta^4 + \frac{\lambda_{\eta h}}{2}\eta^2|H|^2. \tag{2}$$

We assume that CP is conserved, which at the level of the scalar potential simply acts as a Z_2 symmetry on η. This forbids mixing with the Higgs. The difference between Z_2 and CP becomes apparent when one considers non-renormalizable interactions. At dimension 5 the only interactions involving η are

$$\mathcal{L}_{\rm int} = \frac{y_f}{\Lambda_f}\eta(i\overline{f_L}Hf_R + \text{h.c.}) + \frac{c_B}{\Lambda_g}\frac{g'^2}{16\pi^2}\eta B_{\mu\nu}\tilde{B}^{\mu\nu} + \frac{c_W}{\Lambda_g}\frac{g^2}{16\pi^2}\eta W^a_{\mu\nu}\tilde{W}^{a\mu\nu} + \frac{c_g}{\Lambda_g}\frac{\alpha_s}{4\pi}\eta G^a_{\mu\nu}\tilde{G}^{a\mu\nu}, \tag{3}$$

where y_f is the Yukawa coupling of the fermion f and c_B, c_W, and c_g are parameters. For simplicity we supress all fermion operators by a common scale Λ_f and all gauge field operators by a common

final state	scaled
$t\bar{t}$	2.1 pb
$b\bar{b}$	5.6 pb
$Z\gamma$	13 fb
ZZ	56 fb
WW	220 fb
jj	9.4 pb
$\ell^+\ell^-$	5.2 fb
hh	150 fb

Table 3. Observed LHC limits at 13 TeV on $\sigma \times \mathcal{BR}$ rescaled from 8 TeV using the gg parton luminosity [27].

scale Λ_g. These scales can of course be different and it is straightforward to generalize Eq. (3).[2] The normalization we use is $\tilde{B}^{\mu\nu} = \epsilon^{\mu\nu\alpha\beta} B_{\alpha\beta}$.

Notice that loops of SM fermions will already contribute to the interactions between the pseudoscalar and gauge boson pairs. The parameters c_B, c_W, and c_g in Eq. (3) denote contributions in addition to those from SM loops. As we are particularly interested in the diphoton rate, we define the parameter $c_\gamma = c_B + c_W$ which denotes the additional UV contribution to $\eta F_{\mu\nu}\tilde{F}^{\mu\nu}$.

One possibility for UV physics that could generate the dimension 5 operators above are heavy vector-like particles. In this case, one needs to be careful that the new particles do not lead to additional signals that would rule out the pseudoscalar explanation. For instance, requiring the new particles to be heavier than half the pseudoscalar mass protects against large branching ratios to these new particles. The limit where the new particles are just above threshold is interesting as the loop functions are maximal at threshold and could lead to sizable effects. In this work, these effects are parametrized with the aforementioned operator coefficients.

After fixing the pseudoscalar mass to 750 GeV, the parameter space consists of two dimensionful parameters Λ_f and Λ_g and three dimensionless parameters c_B, c_W, and c_g. One can see from the fact that $c_\gamma = c_B + c_W$ that the diphoton coupling can be increased by enhancing either the $\eta B_{\mu\nu}\tilde{B}^{\mu\nu}$ operators or the $\eta W^a_{\mu\nu}\tilde{W}^{a\mu\nu}$ operator. Increasing c_W will increase the WW coupling as well. In this work we set $c_W = 0$ for simplicity such that branching ratio to WW vanishes and WW resonance searches are not constraining. The parameter space is $(\Lambda_f, \Lambda_g, c_\gamma, c_g)$.

It is also interesting to study the case where $c_W \neq 0$. When this is the case, WW resonances searches become constraining in addition to constraints already from $Z\gamma$ and ZZ. While one can select combinations of c_B and c_W to set any of the branching ratios to $Z\gamma$, ZZ, or WW, to zero, the other two are necessarily non zero. In this sense, a generic prediction of the diphoton signal is a signal in two or more of the corresponding diboson channels. In Fig. 1 we show the branching

[2] Although one should note that in our parametrization the difference in gauge scales can be absorbed into c_B, c_W, and c_g.

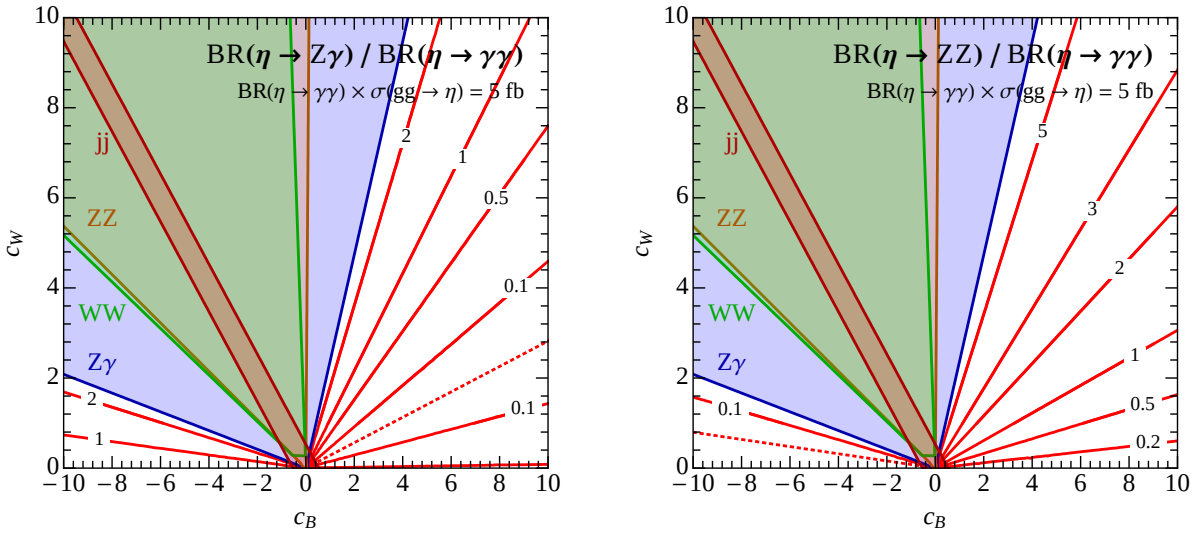

Figure 1. Branching ratio to $Z\gamma$ (left) and ZZ (right) normalized to the diphoton branching ratio. The signal rate is fixed to 5 fb and the colored regions are excluded by 8 TeV diboson searches. The dotted red line shows where the branching ratio vanishes.

ratio to $Z\gamma$ (left) and ZZ (right) normalized to the diphoton branching ratio. In the plot Λ_f is decoupled and consequently $t\bar{t}$ searches are not relevant.

Partial Widths

Given the interactions in Eq. (3) we can compute the partial decay widths. We only show the most relevant which are $t\bar{t}$, gg, $\gamma\gamma$, and to a lesser extent, $b\bar{b}$.

$$\Gamma_{t\bar{t}} = \frac{N_c}{8\pi}\frac{m_t^2}{\Lambda_f^2} m_\eta \sqrt{1-\frac{4m_t^2}{m_\eta^2}}, \tag{4a}$$

$$\Gamma_{b\bar{b}} = \frac{N_c}{8\pi}\frac{m_b^2}{\Lambda_f^2} m_\eta \sqrt{1-\frac{4m_b^2}{m_\eta^2}}, \tag{4b}$$

$$\Gamma_{gg} = \frac{1}{2\pi}\left(\frac{\alpha_s}{4\pi}\right)^2 \frac{m_\eta^3}{\Lambda_f^2}\left|A_-(\tau) + 2c_g\frac{\Lambda_f}{\Lambda_g}\right|^2, \tag{4c}$$

$$\Gamma_{\gamma\gamma} = \frac{1}{4\pi}\left(\frac{\alpha}{4\pi}\right)^2 \frac{m_\eta^3}{\Lambda_f^2}\left|N_c Q_t^2 A_-(\tau) + 2c_\gamma\frac{\Lambda_f}{\Lambda_g}\right|^2, \tag{4d}$$

where $A_-(\tau)$ is the pseudoscalar loop function

$$A_-(\tau) = \tau f(\tau), \qquad \tau = \frac{4m_f^2}{m_\eta^2}, \tag{5}$$

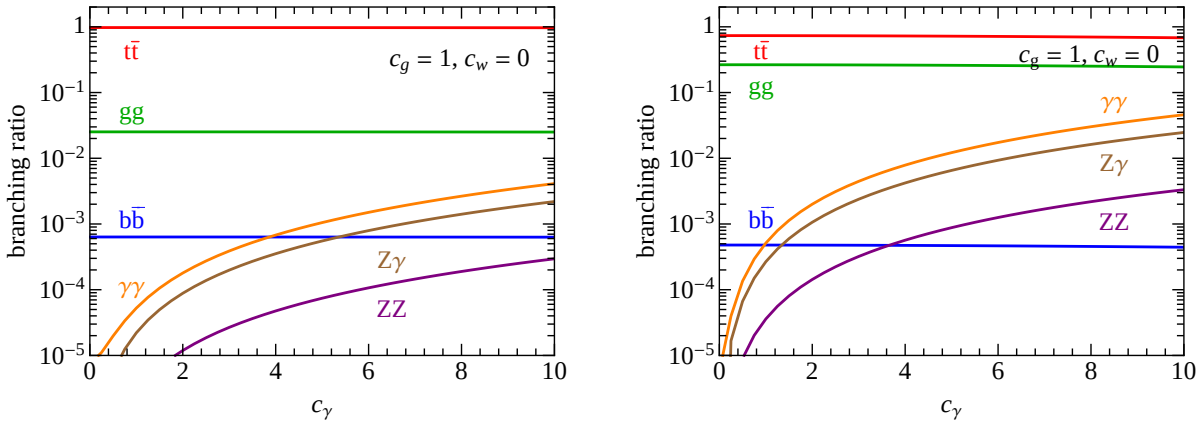

Figure 2. Branching ratios of the pseudoscalar as a function of c_γ which parameterizes UV contributions to the pseudoscalar-photon-photon interactions. The parameters used are $\Lambda_g = 500$ GeV and $\Lambda_f = 750$ GeV (left) and $\Lambda_f = 3$ TeV (right).

and the function $f(\tau)$ is given by

$$f(\tau) = \theta(\tau - 1)\arcsin^2\left(\frac{1}{\sqrt{\tau}}\right) - \theta(1-\tau)\frac{1}{4}\left(\log\frac{1+\sqrt{1-\tau}}{1-\sqrt{1-\tau}} - i\pi\right)^2 . \tag{6}$$

The branching ratios to $Z\gamma$, WW, and ZZ are correlated due to SU(2) gauge invariance. In the limit where we neglect the top loop (which is appropriate in the relevant parameter space) and $c_W = 0$ the ratios are[3]

$$\mathcal{BR}(\gamma\gamma) : \mathcal{BR}(Z\gamma) : \mathcal{BR}(ZZ) : \mathcal{BR}(WW) = 1 : 2t_w^2 : t_w^4 : 0. \tag{7}$$

From Table 3 one can see that for the appropriate diphoton signal, none of the diboson channels are constraining.

In Fig. 2 we show the branching ratios as a function of c_γ for two values of $\Lambda_f = 750$ GeV and $\Lambda_f = 3$ TeV while $\Lambda_g = 500$ GeV and $c_g = 1$. We see that $t\bar{t}$ dominates the branching ratio unless it is supressed by a very large Λ_f value. The branching ratios to $Z\gamma$ and ZZ are estimated by only including their contribution from c_γ and neglecting the top loop contribution to their partial widths.

From Eq. (4) one can quickly estimate the width to be

$$\frac{\Gamma}{m_\eta} \simeq \frac{N_c}{8\pi}\frac{m_t^2}{\Lambda_f^2} \simeq 10^{-2}\left(\frac{600\text{ GeV}}{\Lambda_f}\right)^2 . \tag{8}$$

The pseudoscalar tends to be narrow especially when Λ_f becomes very large.

[3]Recall that this only holds when $c_W = 0$.

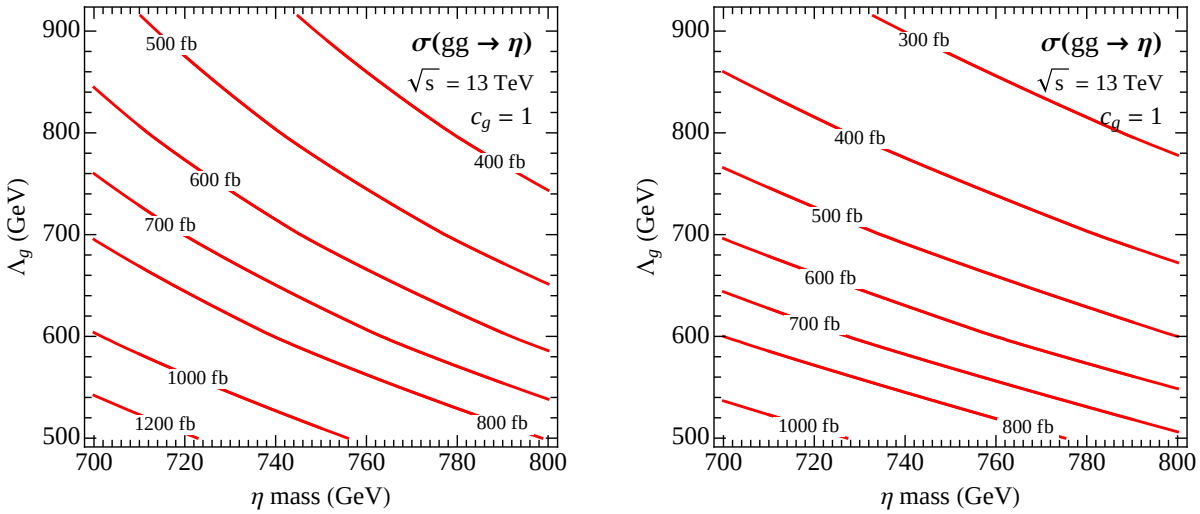

Figure 3. The production cross section of the pseudoscalar as a function of the mass and Λ_g using $\Lambda_f =$ 750 GeV (left) and $\Lambda_f = 3$ TeV (right).

Production rate

From the branching ratios, one can see that the η is produced in gluon fusion. We show the total production cross section as a function of mass and the gauge field scale Λ_g in Fig. 3 for $\Lambda_f =$ 750 GeV (left) and $\Lambda_f = 3$ TeV (right). The only SM fermion we include in the loop is the top quark. We compute the pseudoscalar cross section at NNLO using HIGLU [28] and rescale the cross section to account for an additional gluon fusion contribution via $c_g = 1$. The value of Λ_g controls the relative rate due to the additional dimension 5 contribution.

Simple estimates of the production rate are useful and straightforward to obtain using information provided by the Higgs working group [29] which provides the production rates for heavy Higgses produced in gluon fusion as a function of mass at 8 TeV. First, one needs to account for the difference between scalar and pseudoscalar production. At leading order difference can be obtained by the ratio of loop functions

$$\sigma_\eta = \left| \frac{3}{2} \frac{A_-(4m_t^2/m_\eta^2)}{A_+(4m_t^2/m_\eta^2)} \right|^2 \sigma_H, \tag{9}$$

where $A_+(\tau)$ is the scalar loop function

$$A_+(\tau) = \frac{3}{2}\tau(1 + (1-\tau)f(\tau)). \tag{10}$$

At 750 GeV this ratio works out to be $\simeq 1.45$. Next, one can rescale the 8 TeV rates to 13 TeV by the parton luminosities which is 4.7 for a gg initial state [27]. Finally one needs to account for the prefactor of the pseudoscalar-top coupling in Eq. (3) relative to the Higgs-top coupling in the standard model. Compiling these numbers together and rescaling from the NNLL QCD + NLO

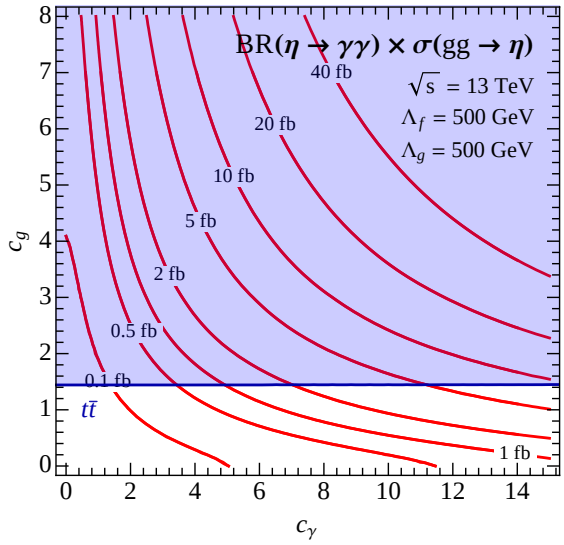

Figure 4. The diphoton rate at 13 TeV using $\Lambda_f = 500$ GeV and $\Lambda_g = 500$ GeV. The blue region is excluded by $t\bar{t}$ searches.

electroweak 8 TeV rate, one finds the rate at 13 TeV to be (for $c_g = 0$)

$$\sigma_\eta(750\text{ GeV})\Big|_{c_g=0} = \left(\frac{v}{\Lambda_f}\right)^2 \times 1.0\text{ pb}. \tag{11}$$

Therefore given a mild suppression from $(v/\Lambda_f)^2$ and a diphoton branching ratio of $\sim 10^{-3} - 10^{-2}$ one can see that the diphoton rate will be $\mathcal{O}(5\text{ fb})$ as is needed to explain the excess. Allowing for a non vanishing c_g the above result is then rescaled (and typically enhanced) by the ratio of the partial width to gluons in the two cases, $\Gamma_{gg}(c_g)/\Gamma_{gg}(c_g = 0)$.

The diphoton rate is computed in Fig. 4 as a function of c_γ and c_g. Clearly c_γ only affects the branching ratio, while c_g both the total rate and the branching ratio since it modifies Γ_{gg}. The blue shaded region indicates where the model is ruled out by 8 TeV searches for $t\bar{t}$ resonances (rescaled to 13 TeV). One can see that a sufficient diphoton rate can be achieved by having either one of c_γ or c_g to be sizable, but because c_g increases the total rate, the $t\bar{t}$ rate also increases. Dijet searches also constrain $c_g < 6$ and $Z\gamma$ searches constrain the diphoton rate to be less than 20 fb. These are not shown in Fig. 4 since $t\bar{t}$ is stronger than both.

In Fig. 5 we slice the parameter space differently and fix a small contribution to gluon fusion via $c_g = 2$ and look at the dependence on Λ_f. We see that as Λ_f is increased, the top loop contribution to the production shrinks as does the $t\bar{t}$ rate itself. The appropriate rate is still attainable from the c_g and c_γ contributions. Dijet searches are not constraining here because the overall rate is smaller and $Z\gamma$ searches still bound the overall diphoton rate (but is not shown in Fig. 5).

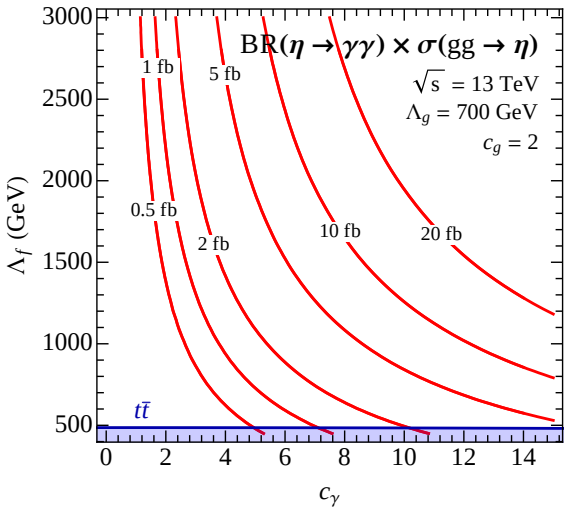

Figure 5. The diphoton rate at 13 TeV using $\Lambda_g = 700$ GeV and $c_g = 2$. The blue region is excluded by $t\bar{t}$ searches.

Results

From Figs. 4 and 5 one can see that it is possible to achieve the observed signal rate of $\sim 1 - 5$ fb. In both cases the strongest constraints come from $t\bar{t}$. Dijet searches are not as sensitive nor are diboson searches as we have used safe value of $c_W = 0$. From the interplay of the effective operators of Eq. (3) two parameter regions that can explain the excess can be identified:

- *A single scale* where $\Lambda_f = \Lambda_g = f$ as in Fig. 4. Given that the scales are not too large, the pseudoscalar to gluon coupling must come mainly from the top loop and one requires a large c_γ value to get the diphoton rate.
- *Suppressed fermions* where $\Lambda_f \gg \Lambda_g = f$ as in Fig. 5. Here the pseudoscalar to top coupling is small enough that $t\bar{t}$ searches are not too constraining. Then gluon fusion can receive a moderate enhancement and the pseudoscalar to photon coupling also only needs a moderate enhancement.

We use the scale f to indicate the scale at which the dimension 5 operators are generated. In the case of a suppressed fermion contribution one can achieve $\Lambda_f \gg \Lambda_g$ either by the fermion contribution being generated at a much higher scale or by a small prefactor such that $\Lambda_f \gg f$. The latter case will be relevant for the composite Higgs case.

Another possibility for a large enough diphoton rate, not mentioned above, is to invoke a large contribution from c_g. To avoid $t\bar{t}$ bounds, it is needed that $\Lambda_f \gg \Lambda_g$, making the coupling of η to tops negligible for all practical purposes. In this limit the rate no longer depends on Λ_f, but only on $(\Lambda_g, c_\gamma, c_g)$. If, for illustration, one fixes $\Lambda_g = 700$ GeV and the diphoton rate to 2 fb, then c_g is the only free parameter since c_γ is determined by the diphoton rate. Then the dijet rate is

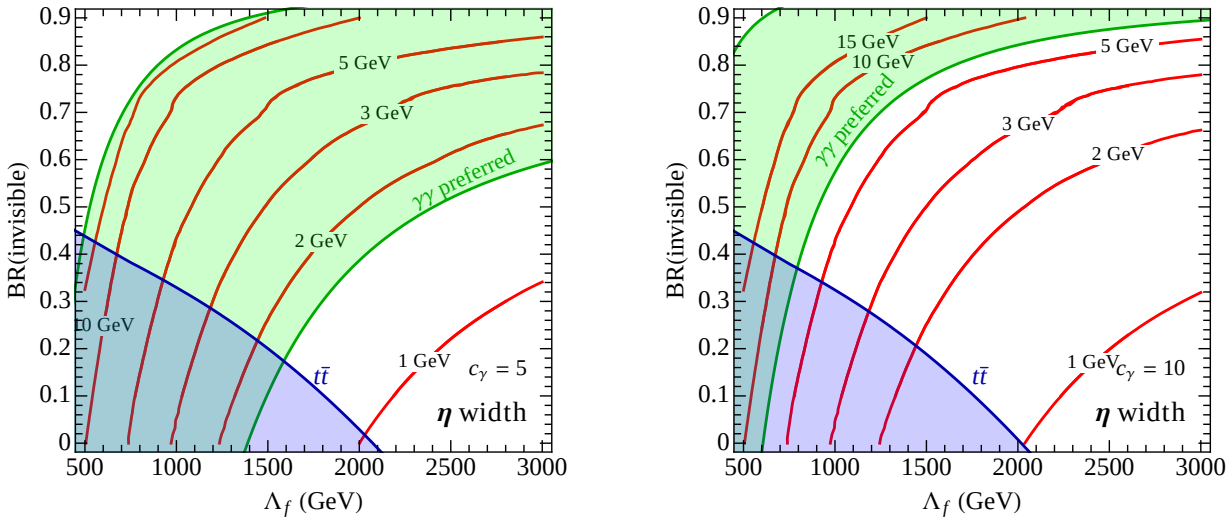

Figure 6. The width of the pseudoscalar as a function of the fermion suppresion scale Λ_f and the invisible branching ratio for $c_\gamma = 5$ (left) and $c_\gamma = 10$ (right). The blue region is excluded by $t\bar{t}$ searches and the green region has a diphoton rate between 1 and 10 fb. The parameters used are $\Lambda_g = 500$ GeV and $c_g = 2$.

$\approx c_g^2$ (400 fb) and the total width is $\approx c_g^2$ (0.04 GeV). We see that in this case, dijet searches bound $c_g \lesssim 4$ and produce a narrow resonance.

Now that we have identified viable regions of parameter space we comment on the width in more detail than Eq. (8). Fig. 6 shows the width as a function of Λ_f and the invisible branching ratio. With only the SM states we have discussed, there is no invisible width and the η tends to be narrow. A wider resonance can be obtained by adding an invisible width.

4 The mass scale of a pseudoscalar

In this section we describe a model in which one can naturally find a pseudoscalar of mass ∼750 GeV. In this model, both the Higgs and the η are pNGBs of a global symmetry. The argument is based on the composite Higgs scenario (for a nice review, see [30]) where the lightest particles of the composite sector are pNGBs. The minimal case identifies the pNGB multiplet with the Higgs multiplet which crucially depends on the global symmetries [31]. One can consider non-minimal scenarios, however, where there are additional light pNGBs which can have various quantum numbers and could even be SM singlets. See [32–36] for previously studied examples.

The general framework

In adding another light scalar, where light is relative to the cutoff, one is once again faced with a hierarchy problem. Just as identifying the Higgs as a pNGB can explain its small mass, the

presence of an additional ∼750 GeV pseudoscalar can be naturally justified if it is also a pNGB of a global symmetry.

In order to accommodate an extra singlet (or extra singlets) we need to go beyond the minimal composite Higgs model [31] and consider a larger global group $\mathcal{G}$. The coset $\mathcal{G}/\mathcal{H}$ then contains the SM Higgs doublet and extra scalars.[4] To control custodial breaking effects that may be induced by the additional scalars it is phenomenologically important to add extra discrete symmetries [36].

As we avoid discussion of a particular model, for our purposes it is sufficient to highlight a few generic facts for models with a pseudoscalar singlet pNGB in addition to the Higgs pNGB multiplet. The full set of pNGBs can be parametrized as

$$U(\Pi) = \exp\left(\frac{i}{f}(\widehat{H} + \eta T_\eta + \ldots)\right), \tag{12}$$

where $\widehat{H}$ is a compact notation for the matrix of pNGBs that will be identified with the SM Higgs and η is the pseudoscalar associated with the broken generator T_η. The $\ldots$ indicate additional pNGBs that could be present.

The standard model $\mathrm{SU}(2)_L \times \mathrm{U}(1)_Y$ gauges a subgroup of the unbroken $\mathcal{H}$. In particular, for η to be a singlet, we must have

$$[T_\eta, T_{\mathrm{SM}}] = 0, \tag{13}$$

where T_{SM} are the generators corresponding to the SM gauge fields. This has relevance for phenomenology, since as it is a singlet the η does not couple to SM gauge fields.

The general couplings of the pNGBs to SM vectors are given by

$$\frac{g_{hVV}}{g^{\mathrm{SM}}_{hVV}} = 1 - \kappa_V \frac{v^2}{f^2} + \mathcal{O}\left(\frac{v^4}{f^4}\right), \qquad \frac{g_{\eta VV}}{g^{\mathrm{SM}}_{hVV}} = 0, \tag{14}$$

where g^{SM}_{hVV} is the Higgs-vector-vector coupling in the standard model and κ_V is an $\mathcal{O}(1)$ coefficient. The pseudoscalar does not couple to SM vectors at tree level. From Eq. (14) one can derive a lower bound on the scale f which is found to be $f \gtrsim 600$ GeV [37,38]. Another important implication of Eq. (14) is that the gauge interactions do not contribute to the one loop generation of a bare mass of the pseudoscalar.

The fermion sector

At this point the couplings between the pNGBs and the SM fermions have not been specified. In this work we focus primarily on the coupling of the pseudoscalar to the top quark because it has the largest Yukawa coupling. The usual generation of masses for SM quarks in composite Higgs models proceeds via the partial compositeness mechanism [39] where the elementary fields couple to operators from the composite sector. Schematically the coupling is

$$y_L \overline{q_L} \cdot U \cdot \Psi + y_R \overline{u_R} \cdot U \cdot \Psi + h.c., \tag{15}$$

[4] A notable case is SO(6)/SO(5) with a Higgs and a pseudoscalar singlet [32], see App. A.

where Ψ represent composite operators and y_L and y_R are related to the fermion Yukawas. While Eq. (15) can be made formally non linearly invariant under $\mathcal{G}$, the SM fermions are embedded in incomplete multiplets of $\mathcal{G}$ which breaks the global symmetries. This breaking in turn generates Yukawa couplings and a potential for the pNGBs. Generically, the Higgs potential always receives a contribution from at least the left handed mixing.

The interactions of the singlet, on the other hand, are model dependent. In particular, if the embeddings of q_L and/or u_R are not eigenstates of the generator T_η, then in general the interactions of Eq. (15) break the shift symmetry of η and contribute to its potential. It is also important to ensure that the embeddings are consistent with our assumption of CP conservation. It has been shown that this can be done in concrete examples [32].

By the appropriate insertions of spurions, y_L and y_R, we can construct the would-be Yukawa term

$$y_t \overline{t_L} h t_R \left(1 + i\kappa_\eta \frac{\eta}{f} + \mathcal{O}\left(\frac{1}{f^2}\right)\right) + h.c., \tag{16}$$

where κ_η is an $\mathcal{O}(1)$ coefficient.

The couplings of the h and η to top quarks is found to be

$$\frac{g_{htt}}{g_{htt}^{\rm SM}} = 1 - \kappa_F \frac{v^2}{f^2}, \qquad \frac{g_{\eta tt}}{g_{htt}^{\rm SM}} = i\frac{v}{f}\kappa_\eta. \tag{17}$$

where $g_{htt}^{\rm SM}$ is the top coupling to the Higgs in the standard model and κ_F is an $\mathcal{O}(1)$ coefficient that depends on the embedding of the fermions. Notice that derivation has been completely general, and the only assumptions have been related to the CP nature of the singlet. It is also manifest that, from the SM perspective, the coupling of the η arises at dimension 5 in complete analogy with the simplified discussion of Sec. 3.

Mass of the pseudoscalar

The mass of the η is determined by the parameter that breaks its shift symmetry. Even though the η is an SM singlet, if the embeddings of q_L or u_R break T_η, then the η's shift symmetry will be broken. Then Eq. (16) will contribute to the η's mass via a contribution to $\lambda_{\eta h}$. This contribution is chirality breaking and involves a Higgs field. There is a chirality preserving contribution that we expect to directly contribute to m_η^2 and arises in the following way.

After having integrated out the composite sector at low energies for u_R we have

$$\overline{u_R}\, \not{p}\, u_R + y_R^2 F_{u_R}(p^2, m_*) \overline{u_R}\, \not{p}\, u_R \left(c_\eta \frac{\eta^2}{f^2} + \dots\right), \tag{18}$$

where F_{u_R} is a form factor that encodes the contribution of the resonances of the strong sector. The poles of F_{u_R} correspond to the masses of the resonances of the strong sector. Here we use m_* to denote the various mass scales of the resonances that we expect below $4\pi f$, but above f.

Note that Eq. (18) is generic for pNGBs that couple to u_R. It is possible that in specific models c_η can vanish due to accidental symmetries [32, 36]. In other models c_η can be proportional to κ_η.

Here we simply consider it to be an $\mathcal{O}(1)$ coefficient. We find a term in the effective potential of the form

$$c_\eta \frac{N_c y_R^2}{4\pi^2} m_*^2 \eta^2. \tag{19}$$

Fixing the top Yukawa, we find

$$y_t \simeq \frac{f}{m_*} y_L y_R \tag{20}$$

and taking $y_L \sim y_R$ we arrive at the estimate,

$$m_\eta^2 \simeq \frac{N_c y_t}{2\pi^2} \frac{m_*^3}{f}. \tag{21}$$

For reasonable values of the parameters we get the estimate,

$$m_\eta \simeq 750 \text{ GeV} \left(\frac{m_*}{1.3 \text{ TeV}}\right)^{3/2} \left(\frac{600 \text{ GeV}}{f}\right)^{1/2}. \tag{22}$$

Interestingly, this is of the right size. It is worth further emphasizing that this mass is at the naturalness limit for η since no tuning is required. This is different than for the Higgs where we need to tune a different combination of coefficients involving the left handed quarks and gauge fields to successfully achieve electroweak symmetry breaking, $v \ll f$.

In this respect, we usually expect a ratio given by

$$\frac{m_\eta}{m_h} \sim \sqrt{\frac{g_*}{y_t}} \frac{f}{v}. \tag{23}$$

Notice that the usual tuning in composite Higgs models requires $g_* \simeq m_*/f \simeq \mathcal{O}(1)$, *i.e.* top partners within reach of the LHC. The same prediction derived from the Higgs mass is true in this model from the η mass. Models of this type, where the mass of the new resonance is natural and linked to the explanation of size of the Higgs mass, seem to deserve further attention even if one has to introduce new ingredients on top of the minimal models.

Interactions of the singlet

In order to connect the composite η with the results of Sec. 3 we comment on the size of c_γ/Λ_g. We start with the top coupling, which from Eq. (17), tells us that tops will couple to the pseudoscalar with a v/f suppression according to

$$\frac{1}{\Lambda_f} \simeq \frac{\kappa_\eta}{f}. \tag{24}$$

In the limit where the η is the lightest new state, the loop induced couplings to gluons and photons are dominated by top contributions.

In the composite sector there are particles (the top partners) charged under both SU(3) and electromagnetism that can also run in the loop. From the view of the composite sector, η is a NGB which means that any shift breaking interaction with top partners must go through an elementary composite mixing. For an estimate, we note that each power of η comes with at least one power

of $y \sim y_R \sim y_L$. Given the symmetries of the strong sector, some of these corrections can have further suppressions. For estimates see App. A.

The challenge of finding large enough c_γ presents itself from the fact that top partner searches have been performed and it seems difficult to evade a bound of ∼700 GeV (see for example [40,41]) and go into a region where the loop functions are enhanced. A similar scaling is expected for the top partner contribution to c_g (without the color and electric charge factors).

It is possible that the global (non-linearly realized) symmetry of the strong group is anomalous. In the case where the generator associated to η has non-vanishing anomaly coefficients with two SM gauge bosons, one can have dimension 5 operators in complete analogy with Eq. (3). The simplest scenario with a light singlet, SO(6) $\simeq$ SU(4), can have global anomalies (SU(4)^3) although with $c_\gamma = 0$ (see App. A).

Other coset spaces can have additional singlets, an example (that suffers custodial breaking and hence is tuned) is SU(3)×U(1)$_X$ / SU(2)$_L$×U(1)$_Y$ [42,43]. The NGBs are in the $\mathbf{2}_{\pm 1/2} + \mathbf{1}_0$ of SU(2)$_L$×U(1)$_Y$. In this case $T_\eta \sim \mathrm{diag}(0,0,1)$. The presence of the U(1)$_X$ allows for a correct hypercharge assignment and the NGBs have charge $X = -1/3$. Hypercharge is defined as $Y = (1/2\sqrt{3})\lambda_8 + X$, where λ_a are the Gell-Mann matrices. In this case $T^2_{\rm em}$ has no particular structure and $\mathrm{tr}[T_\eta T^2_{\rm em}] \neq 0$ in general. At low energies this can manifest itself into an anomalous contribution in the form

$$n_\gamma \frac{\alpha}{4\pi}\frac{\eta}{f} F_{\mu\nu}\tilde{F}^{\mu\nu}, \tag{25}$$

which can help numerically to get a sizable decay to photon pairs. Other choices of global groups could give the same contribution (finding these groups could be a direction of further study), and more exotic groups can also contain color anomalies, hence a contribution to c_g. Finally, notice that in this case the anomaly coefficient is not suppressed by SM couplings.

Results

As a brief summary of the possibilities discussed, we comment on two specific cases, both using a moderate scale $f \sim 600$ GeV, as is suggested by Higgs coupling measurements and naturalness considerations. In particular, given the notation of Eq. (3) we consider $\Lambda_g = f$ and $\Lambda_f = f/\kappa_\eta$ where κ_η is defined in Eq. (17). We leave c_γ and c_g as free parameters, having in mind the possible size as suggested by the previous estimates.

- κ_η is $\mathcal{O}(1)$. In this case where $\Lambda_f = \Lambda_g = f$ in order to sufficiently enhance the diphoton rate a large anomalous contribution to the diphoton coupling seems necessary.

- κ_η is reduced. Then $\Lambda_f > \Lambda_g = f$ and we can be in the case where $\Lambda_f \simeq 3$ TeV where only moderate values of c_γ and c_g are required (see Fig. 5). This is probably still difficult to achieve in the minimal realizations of composite Higgs which only include tops and top partners.

Both of these cases can be visualized in Fig. 7, where we have fixed $c_\gamma = 2$ and $c_g = 2$. Near the top at $\kappa_\eta \simeq 1$ the rate is too low with c_γ and $t\bar{t}$ forces f to start to become large. For small κ_η both the diphoton rate is sufficient and f can be near the preferred value.

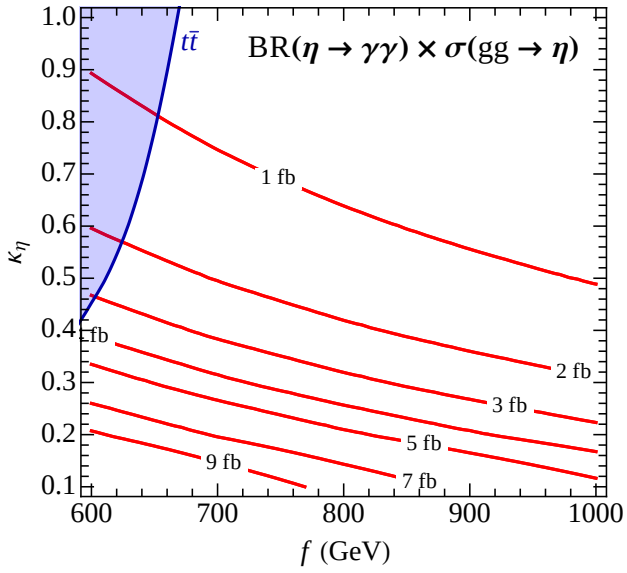

Figure 7. The diphoton rate at 13 TeV for the composite Higgs scenario. The parameters $c_g = 2$ and $c_\gamma = 2$ are used.

5 Alternative explanations

While we have focused on the case of a pseudoscalar resonance, there are obviously a number of possible explanations. The general obstacles that models face were also shared in the pseudoscalar case which are boosting the $\gamma\gamma$ branching ratio to $\sim 10^{-2}$ and avoiding constraints from WW, ZZ, $Z\gamma$, and hh searches. In fact, a nice feature of the pseudoscalar explanation is that symmetries enforce a loop level coupling to both photons and transverse vector bosons, easily evading diboson constraints.

In this section, we briefly outline two other scenarios that could be plausible, namely a spin-0 scalar resonance and a spin-2 resonance. There are other scenarios one can envisage which we do not comment on at all. One example of this would be a 750 GeV particle decaying to two $\mathcal{O}(100$ MeV) particles that each decay to photon pairs. The large boost of the light particles then cause the pair of photons to be detected as a single photon.

5.1 Scalar resonance

A model very similar to the pseudoscalar is a scalar singlet s added to the SM. While assuming CP allowed us to restrict the pseudoscalar from mixing with the SM, we do not have such a symmetry for the scalar (since Z_2 is not useful in this context). In any case, it is possible to assume that the only couplings of the scalar s to the SM are through $F_{\mu\nu}F^{\mu\nu}$ and $G^a_{\mu\nu}G^{\mu\nu a}$, possibly induced by heavy vector-like fermions (see *e.g.* [41]). As discussed in Sec. 3 we find it useful to work below the

scale of the new fermions (in order to avoid decays to them).[5] This model is parametrized by only two interactions (for simplicity, we neglect here constraints from $Z\gamma$, see Sec. 2)

$$\mathcal{L} = \frac{\alpha}{4\pi}\frac{s}{\Lambda_F}F_{\mu\nu}F^{\mu\nu} + \frac{\alpha_s}{4\pi}\frac{s}{\Lambda_G}G^a_{\mu\nu}G^{\mu\nu a}. \tag{26}$$

The overall rate is a function of Λ_G and can be estimated by rescaling the SM rate (similar to Sec. 3)

$$\sigma_s(750\text{ GeV}) = \left(\frac{v}{\Lambda_G}\right)^2 \times 1.25\text{ pb}. \tag{27}$$

The branching ratios are functions of both scales (and gauge couplings) and are

$$\begin{aligned}\mathcal{BR}_{s\to gg} &= \frac{8\alpha_s^2}{8\alpha_s^2 + \alpha^2(\Lambda_G/\Lambda_F)^2},\\ \mathcal{BR}_{s\to\gamma\gamma} &= \frac{\alpha^2(\Lambda_G/\Lambda_F)^2}{8\alpha_s^2 + \alpha^2(\Lambda_G/\Lambda_F)^2},\end{aligned} \tag{28}$$

which can give $\mathcal{BR}_{s\to\gamma\gamma} \sim 10^{-2}$ when Λ_G is sufficiently larger than Λ_F. Then one needs to adjust the cross section with Λ_G where the right value is $\Lambda_G/v \simeq 5$. A full analysis would involve a study of the heavy fermions, including their impact on the running of gauge and Yukawa couplings (which is especially important if the two loop induced effects on the Higgs quartic are large). Such studies are model dependent but would allow one to make concrete predictions for accompanying signals.

5.2 Spin-2 resonance

There are no obstructions for spin-2 particles to decay to photon pairs. Here we consider a hypothetical massive spin-2 particle $\rho_{\mu\nu}$ with a mass m_ρ that couples to the SM stress energy tensor. While it is debatable whether such a light spin-2 particle could be the first observed state (*e.g.* this is not the case in QCD), we explore this possibility with a very pragmatic approach.

Consider a spin-2 Lagrangian with a Fierz-Pauli mass term (as is automatically implied by the Kaluza Klein reduction of 5 dimensional models, see [44] for a review)

$$\mathcal{L} = \mathcal{L}^{\text{FP}}_{\text{spin}-2} + \frac{1}{\Lambda_G}\rho_{\mu\nu}T_B^{\mu\nu} + \frac{1}{\Lambda_F}\rho_{\mu\nu}T_F^{\mu\nu}, \tag{29}$$

where $\rho_{\mu\nu}$ is canonically normalized. We have also separated the interactions with the gauge fields and the Higgs $T_B^{\mu\nu}$ from the stress energy tensor of fermions $T_F^{\mu\nu}$. Other separations could be possible, but for simplicity we use this distinction.

In the limit $m_\rho \gg m_{\text{SM}}$ the form of the partial widths are dominated practically by counting degrees of freedom, since the leading contributions from mass terms are proportional to $T^{\mu\nu} \sim \eta^{\mu\nu}$ and thus vanish onshell. The partial decays widths are [45]

$$\Gamma_{\gamma\gamma} \simeq \frac{m_\rho^3}{80\pi\Lambda_G^2}, \qquad \Gamma_{gg} \simeq 8\Gamma_{\gamma\gamma}, \qquad \Gamma_{ZZ} \simeq \frac{13}{12}\Gamma_{\gamma\gamma}, \qquad \Gamma_{WW} \simeq \frac{13}{6}\Gamma_{\gamma\gamma}, \qquad \Gamma_{hh} \simeq \frac{1}{12}\Gamma_{\gamma\gamma}, \tag{30}$$

[5] As the heavy fermions must be colored to couple to gluons, they also must be unstable because they are colored. Additional model building is necessary to ensure these are phenomenologically viable and will likely lead to specific predictions of the mass or couplings.

and

$$\Gamma_{\ell\ell} \simeq \frac{m_\rho^3}{160\pi\Lambda_F^2}, \qquad \Gamma_{qq} \simeq N_c\Gamma_{\ell\ell}. \tag{31}$$

If the ratio of couplings is $\Lambda_G/\Lambda_F \ll 1$ the dominant production channel could be gluon fusion. Given that the ratios among boson couplings have been fixed, the diphoton branching ratio is

$$\mathcal{BR}_{\rho\to\gamma\gamma} \simeq \frac{3}{37} + \mathcal{O}\left(\frac{\Lambda_G^2}{\Lambda_F^2}\right) \sim 8\%. \tag{32}$$

The total rate should thus be $20-40$ fb. Due to the sensitivity of dilepton searches, the branching ratios of leptons must be $\lesssim 1\%$ which justifies the approximation made. The total rate for fixed m_ρ then is a function of Λ_G which can be selected to achieve the correct rate to explain the excess.

6 Conclusions

In this paper we considered a possible framework that can explain the excess reported by ATLAS and CMS in the search for diphoton resonances and and explored the consequences. Given the challenges imposed by a resonance observed first in its decay to diphoton, a channel with a notoriously small branching ratio, we focused on a pseudoscalar resonance. This is a scenario where we avoid the very strong limits posed by dilepton and diboson searches (see Table 3). As discussed, a proposed singlet pseudoscalar couples to SM particles only at the non-renormalizable level to operators that are SM singlets and CP odd. This list is rather constrained and the leading interactions are to tops, gluons, and photons. We emphasized two possible limits of the effective description. Particles of other natures, like a CP even scalar or a spin-2 particle also face numerous constraints.

The first limit, a "natural scenario", could be offered by new physics in which the suppression scale is common for all operators, thus establishing the coupling of the singlet to the SM top as the leading interaction. In this limit we showed that searches for $t\bar{t}$ resonances from 8 TeV data already constrain part of the parameter space. Moreover, in this case to match the diphoton rate, the coupling to photons requires a sizable contribution from new physics. This case seems difficult to realize in composite Higgs models without adding new states in addition to those from the composite sector. As we have stressed, the challenge is to get a sufficiently large branching ratio to diphoton which could be done by relying on anomalous couplings which are allowed if the global symmetries of the composite sector are anomalous.

The second limit is to assume that the new physics responsible for the effective operators only produces a sizable coupling to the field strengths of the gauge bosons (and not to the fermions). In this case the $t\bar{t}$ constraint is avoided and the excess can be reproduced by invoking sizable effects in $G^a_{\mu\nu}\tilde{G}^{\mu\nu a}$. Then the suppression scale of $\sim$3 TeV for the fermion operator (and $\mathcal{O}(1)$ coupling) could be sufficient to explain the excess. Since only moderate values of c_γ and c_g are required, fewer new states are needed relative to the previous case. One drawback is that even if this scenario was realized in the composite picture, one still requires a moderate tuning of the size of the coupling between the singlet and the top.

A common aspect to both viable scenarios is that the diphoton excess can only be explained if a sector of new particles and interactions is present at a relative low scale, comparable or possibly

even lower than 750 GeV. In particular the presence of colored and electroweakly charged states seems unavoidable. Moreover, in the case of composite models with anomalous contributions to the decay channels, one expects colored (and possibly long lived) pions that might be accessible at LHC. The diphoton excess represents an exciting prospect as Run 2 has only just started. Forthcoming data will tell us more.

Acknowledgements

The authors would like to thank Nima Arkani-Hamed, Gustavo Burdman, Raffaele Tito D'Agnolo, and David Pinner for useful conversations. AT thanks Marco Farina and Michele Redi for interesting comments. ML is supported by a Peter Svennilson Membership at the Institute for Advanced Study, AT is supported by an Oehme Fellowship, and LTW is supported by DOE grant DE-SC0013642.

The Arxiv excess The diphoton excess has already received much attention [46–55]. For issues related to a possible interpretation in composite Higgs scenarios [54].

A SO(6)/SO(5) model

In this appendix we derive some useful formulas for the SO(6)/SO(5) composite Higgs model with a Higgs and a pseudoscalar η. This section is intended to clarify some of the estimates and arguments given in Sec. 4 with the aid of an explicit case.

A.1 The gauge sector

The standard model $\mathrm{SU}(2)_L \times \mathrm{U}(1)_Y$ is embedded in an SO(4) subgroup of the unbroken SO(5), under which the η is an exact goldstone. The "pions" of the coset space can be organized in the matrix

$$\Pi = \sqrt{2}(h^i T^i + \eta T_\eta) = \begin{pmatrix} \mathbf{0}_4 & 0 & \vec{h} \\ 0 & 0 & \eta \\ \hline -\vec{h}^T & -\eta & 0 \end{pmatrix}, \tag{33}$$

where T^i $(i = 1, 2, 3, 4)$ and T_η are the broken generators of SO(6). For convention we gauge the $\mathrm{SU}(2)_L \times \mathrm{U}(1)_Y$ subgroup in the upper left 4×4 block, which is consistent with the assumption of η being a SM singlet. We then define the vector $\Sigma_i \equiv [\exp(i\Pi/f)]_i{}^6$ as (where now $i = 1, \ldots, 6$)

$$\Sigma^T = \frac{\sin(\sqrt{h^2+\eta^2}/f)}{\sqrt{h^2+\eta^2}/f}(\vec{h}, \eta, f\cot(\sqrt{h^2+\eta^2}/f)), \tag{34}$$

where $h^2 = \vec{h}^2$. We perform a field redefinition [32]

$$\vec{h} \leftarrow f\frac{\vec{h}}{\sqrt{h^2+\eta^2}}s, \qquad \eta \leftarrow f\frac{\eta}{\sqrt{h^2+\eta^2}}s, \tag{35}$$

where $s = \sin(\sqrt{h^2+\eta^2}/f)$. In terms of the new fields, the goldstone multiplet is

$$\Sigma^T = (\vec{h}, \eta, \sqrt{f^2 - h^2 - \eta^2}), \tag{36}$$

which leads to the following effective lagrangian (in unitary gauge)

$$\begin{aligned} \mathcal{L} &= \frac{1}{2}(D^\mu \Sigma)^T D_\mu \Sigma \\ &= \frac{1}{2}(\partial_\mu h)^2 + \frac{1}{2}(\partial_\mu \eta)^2 + \frac{1}{2f^2}(h\partial_\mu h + \eta \partial_\mu \eta)^2 + \frac{g^2}{4} h^2 W^a_\mu W^{\mu a} + \dots \end{aligned} \tag{37}$$

In this basis it is manifest that $\langle h \rangle = v = 246$ GeV and the η does not contribute to the electroweak vacuum expectation value. From Eq. (37), however, we see that after electroweak symmetry breaking there will be a non canonically normalized kinetic term for h. The following shift

$$h \to v + \sqrt{1 - \frac{v^2}{f^2}}\, h, \qquad \eta \to \eta, \tag{38}$$

restores canonical normalization and allows us to compute the couplings to vectors

$$\frac{g_{hVV}}{g^{\rm SM}_{hVV}} = \sqrt{1 - \frac{v^2}{f^2}}, \qquad \frac{g_{\eta VV}}{g^{\rm SM}_{hVV}} = 0, \tag{39}$$

where $g^{\rm SM}_{hVV}$ is the SM coupling.

Anomalies

The global symmetry SO(6) $\simeq$ SU(4) can have anomalies. In terms of the SU(4) generators the embedding of the SM is

$$T^a_L \sim \begin{pmatrix} \sigma^a & & \\ & & \\ & & \end{pmatrix}, \qquad T^a_R \sim \begin{pmatrix} & & \\ & \sigma^a & \\ & & \end{pmatrix}, \qquad T_\eta \sim \begin{pmatrix} \mathbb{I} & & \\ & & \\ & & -\mathbb{I} \end{pmatrix}, \tag{40}$$

while $\mathrm{U}(1)_X$ is an external abelian factor. Global anomalies of $\mathrm{SU}(4)^3$ induce anomalous couplings of the η to SM gauge fields, with the anomaly coefficients of $\mathrm{SU}(2)_L$, c_W, and hypercharge, c_B, fixed by the embedding of the SM inside SU(4) to satisfy $c_W + c_B = 0$, as can be explicitly checked. Indeed, the generator of the singlet is $T_\eta \sim \mathrm{diag}(1,1,-1,-1)$ while $T_{\rm em} \sim \mathrm{diag}(1,-1,1,-1) + q_X \mathbb{I}$, where q_X is a charge of an additional $U(1)_X$.

A.2 The fermion sector

As discussed in Eq. (15) the SM fermions are embedded in incomplete representations of SO(6). More precisely the global group needs to be $\mathrm{SO}(6) \times \mathrm{U}(1)_X$ where SM hypercharge is defined as $Y = X + T^3_R$. Among the several irreducible representations of SO(6), we consider here the $\mathbf{6}_{2/3}$ which decomposes under $\mathrm{SO}(5) \times \mathrm{U}(1)_X$ as a $\mathbf{5}_{2/3} + \mathbf{1}_{2/3} + \mathbf{1}_{2/3}$. Under the $\mathrm{SU}(2)_L \times \mathrm{SU}(2)_R$ the decomposition is

$$\mathbf{6}_{2/3} \to (\mathbf{2},\mathbf{2})_{2/3} + (\mathbf{1},\mathbf{1})_{2/3} + (\mathbf{1},\mathbf{1})_{2/3}. \tag{41}$$

We can embed quark doublet q_L in the bidoublet component, while the u_R can be embedded in a linear combination of the two singlets. An embedding that is consistent with our assumption of CP conservation, also at the level of the composite sector, is

$$q_L^T = \frac{1}{\sqrt{2}}(ib_L, b_L, it_L, -t_L, 0, 0), \qquad u_R^T = (0, 0, 0, 0, i\cos\theta, \sin\theta)\ u_R. \tag{42}$$

Eq. (42) shows that the mixing of q_L does not break the shift symmetry of η (*i.e.* $T_\eta q_L = 0$) while in general the mixing of u_R does break it. Depending on value of θ, which controls the coupling of u_R to η, one can have different scenarios.

For $\theta = \pi/4$, η is an exact goldstone since the mixing respects the $\mathrm{U}(1)_\eta$ symmetry that is generated by T_η. Even though it is a goldstone it still couples to u_R. On the other hand, for $\theta = \pi/2$, the mixing respects a discrete Z_2 symmetry, but η does not couple to fermions. In the discussion in Sec. 4 we implicitly avoided these two limiting cases to ensure a coupling between the η and $t\bar{t}$. Lighter quarks, however, can have different embeddings and one can even choose embeddings to automatically satsify $\theta = \pi/2$ or $\theta = \pi/4$ [56].

The form of the Yukawa term is constrained to be

$$y_t(q_L\Sigma)(\Sigma^T u_R) = \frac{y_t}{\sqrt{2}}\overline{t_L}ht_R\left(\frac{\sqrt{f^2-h^2-\eta^2}}{f^2}\sin\theta + \frac{\eta}{f}i\cos\theta\right) + h.c. \tag{43}$$

Normalizing to the SM Higgs couplings we have the following couplings to fermions for h and η

$$\frac{g_{htt}}{g_{htt}^{\mathrm{SM}}} = \frac{1-{}^{2v^2}/_{f^2}}{\sqrt{1-{}^{v^2}/_{f^2}}}, \qquad \frac{g_{\eta tt}}{g_{htt}^{\mathrm{SM}}} = i\frac{v}{f}\frac{\cot\theta}{\sqrt{1-{}^{v^2}/_{f^2}}}, \tag{44}$$

to be compared with Eq. (17). Notice that since the top mass is proportional to $\sin\theta$ smaller values of $\sin\theta$ will increase the coupling of the top to the pseudoscalar, but will also induce tuning among the parameters of the model.

Other terms can be written with the Σ, an example used in Sec. 4 are chirality preserving operators that can induce a leading contribution to the potential for η, as

$$\overline{u_R}\not{p}\,\Sigma^T\Sigma u_R = \overline{u_R}\not{p}\,u_R(\eta^2\cos^2\theta + (f^2-h^2-\eta^2)\sin^2\theta), \tag{45}$$

which justifies the expression in Eq. (19).

Contributions to c_γ and c_g from top partners

A refined estimate for the UV contribution to c_γ and c_g from the top partners involves the full mass spectrum of the heavy fermions. In order to be explicit, we consider the case where the left handed and right handed elementary quarks each couple to a **6** of SO(6). The **6** decomposes as a **5** + **1**, the states for which we denote as Ψ_5 and Ψ_1, respectively. They lead to the mass terms

$$\mathcal{L} \supset y_L f\overline{q_L}U\Psi_R + y_R f\overline{\Psi_L}Uu_R - m_5\overline{\Psi}_{5L}\Psi_{5R} - m_1\overline{\Psi}_{1L}\Psi_{1R} + h.c. \tag{46}$$

The states of the **6** are

$$\Psi = \frac{1}{\sqrt{2}} \begin{pmatrix} iB - iX_{5/3} \\ B + X_{5/3} \\ iX_{2/3} + iT \\ X_{2/3} - T \\ i\sqrt{2}T_a \\ \sqrt{2}T_b \end{pmatrix}, \tag{47}$$

where under the SM these are (T, B), $(X_{5/3}, X_{2/3})$, T_a, and T_b which are respectively a $\mathbf{2}_{7/6}$, a $\mathbf{2}_{1/6}$, a $\mathbf{1}_{2/3}$, and a $\mathbf{1}_{2/3}$. The upper 5 components comprise Ψ_5 and the lowest is Ψ_1.

The actual calculation of the effective coupling to the field strengths can be simplified using the Higgs low energy theorem that allows us to compute the contribution using only the mass spectrum. In particular, for a top partner Ψ^i we need to know the Yukawa coupling g_i and the mass m_i defined as $ig_i\eta\Psi^i\gamma_5\Psi^i$ and $m_i\Psi^i\Psi^i$. With reference to Eq. (46) we note that m_i is a function of h and η, but given the assumption of CP conservation $m_i = m_i(\eta = 0)$. On the other hand, g_i can be computed from the imaginary part of the mass matrix $\mathcal{M}$ in the background of η, $ig_i = \partial m_i/\partial\eta|_{\eta=0}$. The following relation holds,

$$\sum_i \frac{g_i}{m_i} = \frac{\partial}{\partial\eta} \log\det\mathcal{M} = \frac{1}{f}\frac{\cot\theta}{\sqrt{1 - v^2/f^2}}, \tag{48}$$

where i runs over the fermion states including the SM top. This contribution is equal to the contribution just from the top in Eq. (44) which means that the contribution of fermions much heavier than η vanishes. Notice that differently from the case of the Higgs couplings [57] here the wave function renormalization of the light quarks does not introduce new effects (unless CP is broken).

The overall contribution from top partners is then

$$\frac{c_\gamma}{\Lambda} = \frac{4}{3}\sum_i \frac{g_i}{m_i} A_-(\tau_i) \simeq \frac{1}{f}\cdot\mathcal{O}\left(\frac{m_t}{m_*}\frac{m_\eta^2}{m_*^2}\right) \tag{49}$$

This suggests that one has to deviate from the limit of all heavy top partners, however, as discussed in Sec. 4, it seems challenging to achieve the size needed for c_γ and c_g solely from top partners and comply with the direct limits on their masses.

References

[1] *Search for resonances decaying to photon pairs in 3.2 fb^{-1} of pp collisions at $\sqrt{s}$ = 13 TeV with the ATLAS detector*, Tech. Rep. ATLAS-CONF-2015-081, CERN, Geneva, Dec, 2015.

[2] **CMS Collaboration** Collaboration, *Search for new physics in high mass diphoton events in proton-proton collisions at 13TeV*, Tech. Rep. CMS-PAS-EXO-15-004, CERN, Geneva, 2015.

[3] **ATLAS** Collaboration, G. Aad et al., *Search for high-mass diphoton resonances in pp collisions at $\sqrt{s} = 8$ TeV with the ATLAS detector*, *Phys. Rev.* **D92** (2015), no. 3 032004, [arXiv:1504.05511].

[4] **CMS** Collaboration, C. Collaboration, *Search for High-Mass Diphoton Resonances in pp Collisions at sqrt(s)=8 TeV with the CMS Detector*, .

[5] **CMS** Collaboration, V. Khachatryan et al., *Search for diphoton resonances in the mass range from 150 to 850 GeV in pp collisions at $\sqrt{s} = 8$ TeV*, *Phys. Lett.* **B750** (2015) 494–519, [arXiv:1506.02301].

[6] ATLAS and C. collaborations, *ATLAS and CMS physics results from Run 2*, 2015. http://indico.cern.ch/event/442432/.

[7] **ATLAS** Collaboration, G. Aad et al., *A search for $t\bar{t}$ resonances using lepton-plus-jets events in proton-proton collisions at $\sqrt{s} = 8$ TeV with the ATLAS detector*, *JHEP* **08** (2015) 148, [arXiv:1505.07018].

[8] **CMS** Collaboration, V. Khachatryan et al., *Search for Resonant $\mathrm{t\bar{t}}$ Production in Proton-Proton Collisions at $\sqrt{s} = 8$ TeV*, arXiv:1506.03062.

[9] **CMS** Collaboration, V. Khachatryan et al., *Search for Neutral MSSM Higgs Bosons Decaying into A Pair of Bottom Quarks*, *JHEP* **11** (2015) 071, [arXiv:1506.08329].

[10] **ATLAS** Collaboration, G. Aad et al., *Search for new resonances in $W\gamma$ and $Z\gamma$ final states in pp collisions at $\sqrt{s} = 8$ TeV with the ATLAS detector*, *Phys. Lett.* **B738** (2014) 428–447, [arXiv:1407.8150].

[11] **ATLAS** Collaboration, G. Aad et al., *Search for an additional, heavy Higgs boson in the $H \to ZZ$ decay channel at $\sqrt{s} = 8$ TeV in pp collision data with the ATLAS detector*, arXiv:1507.05930.

[12] **ATLAS** Collaboration, G. Aad et al., *Search for resonant diboson production in the $\ell\ell q\bar{q}$ final state in pp collisions at $\sqrt{s} = 8$ TeV with the ATLAS detector*, *Eur. Phys. J.* **C75** (2015) 69, [arXiv:1409.6190].

[13] **CMS** Collaboration, V. Khachatryan et al., *Search for a Higgs Boson in the Mass Range from 145 to 1000 GeV Decaying to a Pair of W or Z Bosons*, *JHEP* **10** (2015) 144, [arXiv:1504.00936].

[14] **CMS** Collaboration, V. Khachatryan et al., *Search for massive resonances decaying into pairs of boosted bosons in semi-leptonic final states at $\sqrt{s} = 8$ TeV*, *JHEP* **08** (2014) 174, [arXiv:1405.3447].

[15] **ATLAS** Collaboration, G. Aad et al., *Search for production of WW/WZ resonances decaying to a lepton, neutrino and jets in pp collisions at $\sqrt{s} = 8$ TeV with the ATLAS detector*, *Eur. Phys. J.* **C75** (2015), no. 5 209, [arXiv:1503.04677]. [Erratum: Eur. Phys. J.C75,370(2015)].

[16] **ATLAS** Collaboration, G. Aad et al., *Search for new phenomena in the dijet mass distribution using $p-p$ collision data at $\sqrt{s} = 8$ TeV with the ATLAS detector*, *Phys. Rev.* **D91** (2015), no. 5 052007, [arXiv:1407.1376].

[17] **CMS Collaboration** Collaboration, *Search for Resonances Decaying to Dijet Final States at $\sqrt{s} = 8$ TeV with Scouting Data*, Tech. Rep. CMS-PAS-EXO-14-005, CERN, Geneva, 2015.

[18] **ATLAS** Collaboration, G. Aad et al., *Search for high-mass dilepton resonances in pp collisions at $\sqrt{s} = 8$TeV with the ATLAS detector*, *Phys. Rev.* **D90** (2014), no. 5 052005, [arXiv:1405.4123].

[19] **CMS** Collaboration, V. Khachatryan et al., *Search for physics beyond the standard model in dilepton mass spectra in proton-proton collisions at $\sqrt{s} = 8$ TeV*, *JHEP* **04** (2015) 025, [arXiv:1412.6302].

[20] **ATLAS** Collaboration, G. Aad et al., *Search for Higgs boson pair production in the $b\bar{b}b\bar{b}$ final state from pp collisions at $\sqrt{s} = 8$ TeVwith the ATLAS detector*, *Eur. Phys. J.* **C75** (2015), no. 9 412, [arXiv:1506.00285].

[21] **CMS** Collaboration, V. Khachatryan et al., *Search for resonant pair production of Higgs bosons decaying to two bottom quarkantiquark pairs in protonproton collisions at 8 TeV*, *Phys. Lett.* **B749** (2015) 560–582, [arXiv:1503.04114].

[22] **CMS** Collaboration, V. Khachatryan et al., *Search for neutral MSSM Higgs bosons decaying to a pair of tau leptons in pp collisions*, *JHEP* **10** (2014) 160, [arXiv:1408.3316].

[23] **ATLAS** Collaboration, G. Aad et al., *Search for neutral Higgs bosons of the minimal supersymmetric standard model in pp collisions at $\sqrt{s}$ = 8 TeV with the ATLAS detector*, *JHEP* **11** (2014) 056, [arXiv:1409.6064].

[24] **ATLAS** Collaboration, G. Aad et al., *Search for a CP-odd Higgs boson decaying to Zh in pp collisions at $\sqrt{s} = 8$ TeV with the ATLAS detector*, *Phys. Lett.* **B744** (2015) 163–183, [arXiv:1502.04478].

[25] **CMS** Collaboration, V. Khachatryan et al., *Search for dark matter, extra dimensions, and unparticles in monojet events in protonproton collisions at $\sqrt{s} = 8$ TeV*, *Eur. Phys. J.* **C75** (2015), no. 5 235, [arXiv:1408.3583].

[26] **ATLAS** Collaboration, G. Aad et al., *Search for new phenomena in final states with an energetic jet and large missing transverse momentum in pp collisions at $\sqrt{s}$ =8 TeV with the ATLAS detector*, *Eur. Phys. J.* **C75** (2015), no. 7 299, [arXiv:1502.01518]. [Erratum: Eur. Phys. J.C75,no.9,408(2015)].

[27] TWIKI, *SM Higgs production cross sections at 13 - 14 TeV*, 2015. https://twiki.cern.ch/twiki/bin/view/LHCPhysics/CERNYellowReportPageAt1314TeV.

[28] M. Spira, *HIGLU: A program for the calculation of the total Higgs production cross-section at hadron colliders via gluon fusion including QCD corrections*, hep-ph/9510347.

[29] **LHC Higgs Cross Section Working Group** Collaboration, J. R. Andersen et al., *Handbook of LHC Higgs Cross Sections: 3. Higgs Properties*, arXiv:1307.1347.

[30] G. Panico and A. Wulzer, *The Composite NambuGoldstone Higgs*, *Lect. Notes Phys.* **913** (2016) pp.–, [arXiv:1506.01961].

[31] K. Agashe, R. Contino, and A. Pomarol, *The Minimal composite Higgs model*, *Nucl. Phys.* **B719** (2005) 165–187, [hep-ph/0412089].

[32] B. Gripaios, A. Pomarol, F. Riva, and J. Serra, *Beyond the Minimal Composite Higgs Model*, *JHEP* **04** (2009) 070, [arXiv:0902.1483].

[33] J. Serra, *Beyond the Minimal Top Partner Decay*, *JHEP* **09** (2015) 176, [arXiv:1506.05110].

[34] E. Katz, A. E. Nelson, and D. G. E. Walker, *The Intermediate Higgs*, *JHEP* **08** (2005) 074, [hep-ph/0504252].

[35] J. Galloway, J. A. Evans, M. A. Luty, and R. A. Tacchi, *Minimal Conformal Technicolor and Precision Electroweak Tests*, *JHEP* **10** (2010) 086, [arXiv:1001.1361].

[36] J. Mrazek, A. Pomarol, R. Rattazzi, M. Redi, J. Serra, and A. Wulzer, *The Other Natural Two Higgs Doublet Model*, *Nucl. Phys.* **B853** (2011) 1–48, [arXiv:1105.5403].

[37] **ATLAS** Collaboration, T. A. collaboration, *Measurements of the Higgs boson production and decay rates and coupling strengths using pp collision data at s = 7 and 8 TeV in the ATLAS experiment*, .

[38] **CMS** Collaboration, V. Khachatryan et al., *Precise determination of the mass of the Higgs boson and tests of compatibility of its couplings with the standard model predictions using proton collisions at 7 and 8 TeV*, *Eur. Phys. J.* **C75** (2015), no. 5 212, [arXiv:1412.8662].

[39] D. B. Kaplan, *Flavor at SSC energies: A New mechanism for dynamically generated fermion masses*, *Nucl. Phys.* **B365** (1991) 259–278.

[40] O. Matsedonskyi, G. Panico, and A. Wulzer, *On the Interpretation of Top Partners Searches*, *JHEP* **12** (2014) 097, [arXiv:1409.0100].

[41] J. A. Aguilar-Saavedra, R. Benbrik, S. Heinemeyer, and M. Prez-Victoria, *Handbook of vectorlike quarks: Mixing and single production*, *Phys. Rev.* **D88** (2013), no. 9 094010, [arXiv:1306.0572].

[42] R. Contino, Y. Nomura, and A. Pomarol, *Higgs as a holographic pseudoGoldstone boson*, *Nucl. Phys.* **B671** (2003) 148–174, [hep-ph/0306259].

[43] M. Schmaltz, *The Simplest little Higgs*, *JHEP* **08** (2004) 056, [hep-ph/0407143].

[44] K. Hinterbichler, *Theoretical Aspects of Massive Gravity*, *Rev. Mod. Phys.* **84** (2012) 671–710, [arXiv:1105.3735].

[45] T. Han, J. D. Lykken, and R.-J. Zhang, *On Kaluza-Klein states from large extra dimensions*, *Phys. Rev.* **D59** (1999) 105006, [hep-ph/9811350].

[46] K. Harigaya and Y. Nomura, *Composite Models for the 750 GeV Diphoton Excess*, arXiv:1512.04850.

[47] Y. Mambrini, G. Arcadi, and A. Djouadi, *The LHC diphoton resonance and dark matter*, arXiv:1512.04913.

[48] M. Backovic, A. Mariotti, and D. Redigolo, *Di-photon excess illuminates Dark Matter*, arXiv:1512.04917.

[49] A. Angelescu, A. Djouadi, and G. Moreau, *Scenarii for interpretations of the LHC diphoton excess: two Higgs doublets and vector-like quarks and leptons*, arXiv:1512.04921.

[50] Y. Nakai, R. Sato, and K. Tobioka, *Footprints of New Strong Dynamics via Anomaly*, arXiv:1512.04924.

[51] S. Knapen, T. Melia, M. Papucci, and K. Zurek, *Rays of light from the LHC*, arXiv:1512.04928.

[52] D. Buttazzo, A. Greljo, and D. Marzocca, *Knocking on New Physics' door with a Scalar Resonance*, arXiv:1512.04929.

[53] A. Pilaftsis, *Diphoton Signatures from Heavy Axion Decays at LHC*, arXiv:1512.04931.

[54] R. Franceschini, G. F. Giudice, J. F. Kamenik, M. McCullough, A. Pomarol, R. Rattazzi, M. Redi, F. Riva, A. Strumia, and R. Torre, *What is the gamma gamma resonance at 750 GeV?*, arXiv:1512.04933.

[55] S. Di Chiara, L. Marzola, and M. Raidal, *First interpretation of the 750 GeV di-photon resonance at the LHC*, arXiv:1512.04939.

[56] M. Frigerio, A. Pomarol, F. Riva, and A. Urbano, *Composite Scalar Dark Matter*, *JHEP* **07** (2012) 015, [arXiv:1204.2808].

[57] A. Azatov and J. Galloway, *Light Custodians and Higgs Physics in Composite Models*, *Phys. Rev.* **D85** (2012) 055013, [arXiv:1110.5646].